We are IntechOpen, the world's leading publisher of Open Access books Built by scientists, for scientists

6,900
Open access books available

185,000
International authors and editors

200M
Downloads

154
Countries delivered to

Our authors are among the

TOP 1%
most cited scientists

12.2%
Contributors from top 500 universities

CLARIVATE ANALYTICS
BOOK CITATION INDEX
INDEXED

WEB OF SCIENCE™

Selection of our books indexed in the Book Citation Index
in Web of Science™ Core Collection (BKCI)

Interested in publishing with us?
Contact book.department@intechopen.com

Chapter

Power Oscillation Due to Ferroresonance and Subsynchronous Resonance

Salman Rezaei

Abstract

Power oscillation occurs in electrical network due to variety of phenomena. Subsynchronous resonance (SSR) and ferroresonance are the phenomena that cause power oscillation of rotary systems. Ferroresonance is likely to occur due to traversing capacitance line of the system across nonlinear area of transformer saturation curve due to several configurations like breaker failure, voltage transformer connected to grading capacitor circuit breaker, line and plant outage, etc. It causes misshaping the waveforms and frequency difference between two points in the network. Frequency difference (Δf) results in oscillation of power with a swing frequency which is equal to Δf. During SSR, electrical energy is exchanged between generators and transmission systems below power frequency. It happens due to interaction of a series compensated transmission line with a generator. It results in oscillation in the shaft and power oscillation. In addition, SSR causes the magnitudes of voltage and current to increase. Increasing the voltage causes saturation of iron core of transformer or reactor and consequently occurrence of ferroresonance in the presence of series capacitance.

Keywords: power oscillation, ferroresonance, subsynchronous resonance, series compensation, saturation, frequency difference, Manitoba hydro, Mohave plant

1. Introduction

The word ferroresonance was originally expressed in 1920 to explain the phenomenon of two stable fundamental frequency operating points in a series resistor, nonlinear inductor, and capacitor circuit [1]. It has been extensively studied over the past 90 years. Severity of ferroresonance is classified as four categories like fundamental, harmonic, quasi-periodic, and chaotic [2]. Ref [3] explains Conventional configurations which lead in ferroresonance like; voltage transformer (VT) energized through the grading capacitance of open circuit breakers or VT connected to an ungrounded neutral system, circuit breaker failure during opening or closing operation, and power transformer supplied through a long transmission line cable with low short-circuit power [3]. Several methods have been presented to analyze ferroresonance in time and frequency domain. Ref. [4] is concerned with comparing analytical nonlinear dynamics methods with a two-dimensional (2-D) brute-force bifurcation diagram for displaying safety margins in a 2-D parameter space.

Analysis and mitigation of ferroresonant oscillations based on harmonic balance method and bifurcation theory are presented in [5].

Ferroresonance generally occurs in distribution network and is significantly probable in HV systems [6–8]. For instance, plant outage in HV power system is able to change electrical characteristics and parameters in a nonlinear circuit, which may lead in ferroresonance [9].

Impact of ferroresonance has been taken into consideration in wind farm. Ref. [10] presents the scenarios that can lead to ferroresonant circuits in Doubly Fed Induction Generator (DFIG)-based wind parks. Transient and sustained ferroresonance phenomenon in wind farms connected to a power distribution system is analyzed in [11]. Occurrence of ferroresonance causes misshaped waveform of magnitudes with different frequencies. It leads in power oscillation between two points with a certain frequency difference in the network [12]. Ferroresonance is typically damped by using several methods. For instance, installation of permanent resistance in the secondary circuit of distribution transformer; furthermore, replacing VT with CVT causes mitigation of ferroresonance in voltage transformer [6].

The term of SSR has been taken into consideration in the power industry since first experienced in 1970. It results in shaft failure of units at Mohave power plant. The second failure was the real cause of failure recognized as SSR in 1971 [13].

Many investigations have been implemented in analysis and mitigation of SSR. By bifurcation analysis, the stable limit cycle bifurcates to a stable torus and an unstable limit cycle, which connects to a stable limit cycle by a supercritical torus bifurcation [14]. Frequency scanning computes the equivalent resistance and inductance, seen looking into the network from a point behind the stator winding of a generator as a function of frequency [15]. Design and implementation details of an artificial neural network-based SSR are presented in [16]. Time frequency distribution algorithm extracts time variable information about frequency contents from the time domain signal [17].

For the mitigation of SSR, several methods have been presented. STATCOM is used in the transformer bus to damp SSR [18]. Application of gate-controlled series capacitors (GCSC) for reducing stresses due to SSR in turbine-generator shaft is presented in [19]. Fuzzy logic and ANFIS controller-based Static Var Compensation (SVC) for mitigating SSR is explained in [20].

SSR has received considerable attention in the wind farm. SSR analysis on DFIG-based wind farm and optimal adaptive controls to mitigate SSR in wind farm are presented in [21, 22].

SSR causes subharmonic components of electrical quantities to interact with natural frequencies of rotary systems due to series capacitance. It leads in torsional oscillation of the turbo-generator shaft. Torsional oscillation in the shaft results in out of step condition of the generator. It increases the magnitudes of voltage and current. Increasing the voltage causes saturation of transformer and probable occurrence of ferroresonance in a series compensated network [23, 24]. Oscillation due to ferroresonance is superimposed on torsional oscillation in SSR.

In this chapter, theoretical approach of ferroresonance and SSR is presented. Manitoba hydro electrical network has experienced ferroresonant states in 1995 [8]. In addition, it includes long transmission line of about 500 km, which is suitable for series compensation studies [6]. Hence, it is a good example of a case study in this field. The state that results in ferroresonance is simulated in Manitoba hydro system by PSCAD/EMTDC. Power oscillation due to SSR and ferroresonance is presented in HV power system, and results of oscillation are analyzed on electrical and mechanical parameters of rotary systems including hydro generator in Grand Rapids station.

2. Theoretical approach of ferroresonance and subsynchronous resonance

2.1 Ferroresonance

Ferroresonance is a nonlinear resonance, which occurs in presence of a saturable nonlinear inductance and capacitance in a circuit with low resistance. In ferroresonance, the capacitance line crosses inductance characteristic in nonlinear area. It results in presence of abnormally large currents and frequency distortion.

A graphical approach is obtained by calculating the parameters of nonlinear circuits in time domain. For instance, in a typical series, RLC circuit inductor voltage is calculated as follows [6]:

$$V_L = \sqrt{V_h^2 - (I.R)^2} + \frac{I}{\omega C} \tag{1}$$

It is also a nonlinear function of current as follows:

$$V_L = \omega f(I) \tag{2}$$

The inductance in this circuit is a nonlinear element due to the core saturation and hysteresis. The voltage across the capacitance in the circuit is represented as:

$$V_C = I/\omega C \tag{3}$$

where V_h is the total voltage across the circuit. Similarly, the voltage across the inductance can also be expressed as:

$$V_L = V + (I/\omega C) \tag{4}$$

As shown in **Figure 1**, point of intersection of $V_L = \omega f(I)$ and V_C represents the operating point of the circuit. Changing the capacitance of the system causes change in the slope given by *tanα = 1/ωC*. On the other hand, changes in inductance result in an interaction with a wide range of circuit capacitances resulting in existence of several stable steady state responses to any given change of parameter. It causes changes in configuration of the circuit, and so capacitance traverses across nonlinear area of $V_L = \omega f(I)$ curve and results in occurrence of ferroresonance in the circuit.

As was mentioned above, frequency of waveform can be deviated from nominal frequency in ferroresonance so that frequency deviation can be defined as follows
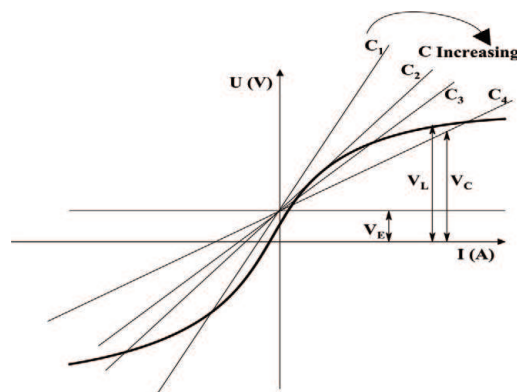

Figure 1.
Diagram of parameters in series RLC ferroresonant circuit.

$$\Delta f = \left| f_{fr} - f_{nom} \right| \tag{5}$$

where f_{fr} is the frequency of waveform in ferroresonance.

Resulted waveform is decomposed to its number of harmonics using fast Fourier transform (FFT). Measurement is done by evaluation of samples, which are taken in specific sampling interval; hence, discrete Fourier transform (DFT) is used with a certain sampling rate to illustrate harmonic components on harmonic spectrum.

$$V_{Lk} = \sum_{n=0}^{N-1} V_{Ln} e^{-j2\pi k \frac{n}{N}} \quad K = 0 \ldots N - 1 \tag{6}$$

N = number of samples.

Then, total harmonic distortion is calculated, and so integer harmonics, which obtained from FFT, are considered in the following formula:

$$THD = \sqrt{\sum_{h=2}^{x} \left(\frac{individual\ (h)}{individual\ (1)} \right)^2} \tag{7}$$

where x is integer harmonics.

In order to determine ferroresonance based on measurement in a logical manner, ferroresonant characteristics must be quantified. THD and Δf are the quantities that are used as criteria to determine ferroresonance of different types (**Table 1**).

As shown in the table, fundamental ferroresonance is detected when frequency of waveform remains at nominal value (Δf is zero) and the value of THD is more than 50%. Harmonic ferroresonance is detected when frequency of waveform is deviated from nominal value and remains constant (Δf is not zero); furthermore, the value of THD is also more than 50%. In most cases, fundamental and harmonic ferroresonance contain odd harmonics; hence, harmonic spectrum is discrete. Quasi-periodic and chaotic modes are determined when $\frac{d\Delta f}{dt}$ is detected and calculated as follow.

$$\frac{d\Delta f}{dt} = T . \frac{\Delta f(t) - \Delta f(t - \Delta t)}{\Delta t} \tag{8}$$

where T is the time constant, $t - \Delta t$ is the previous time step, and Δt is the time step interval.

Furthermore, the value of THD increases more than 100% where chaotic mode contains a continuous harmonic spectrum. As harmonic spectrum is mostly a qualified characteristic, THD and Δf are used to determine ferroresonance modes.

2.2 Subsynchronous resonance

In this section, theoretical aspects of SSR in AC transmission system are explained.

Ferroresonance type	Δf	$\frac{d\Delta f}{dt}$	THD (%)	Harmonic spectrum
Fundamental	Zero	Zero	>50	Discrete
Harmonic	Constant	Zero	>50	Discrete
Quasi-periodic	Variable	Not zero	>100	Discrete
Chaotic	Variable	Not zero	>100	Continuous

Table 1.
Criteria to determine ferroresonance modes.

Loadability of AC transmission line is defined as follows:

$$P = \frac{V_S . V_R}{X_T} sin\delta \tag{9}$$

Series compensation increases transmittable power by adding series capacitors, which decrease total line impedance as follows:

$$X_T = X_L - X_C \tag{10}$$

$$X_T = (1 - S) . X_L \tag{11}$$

Here, S is the compensation degree, which is changed between 0 and 100% defined as follows:

$$S = \frac{X_C}{X_L} \times 100\% \tag{12}$$

The degree of compensation could be 100% theoretically. It may produce large currents in the presence of small disturbances or faults. In other hand, a high level of compensation highlights the problem in protective relays and in voltage profile during fault condition. In a radial series-compensated power system, the electrical resonance frequency is given by the following formula.

$$f_{er} = \pm f_s \sqrt{\frac{X_C}{X_L}} \tag{13}$$

where f_s is power system nominal frequency and X_L is total inductance of the grid.

Current flowing in the grid circulates to the armature winding of the generator and interacts with turbine-generator rotor as subharmonic and super harmonic frequencies. As shown below, the current includes fundamental component (grid frequency), and another sinusoidal components are determined by existing elements in the grid [25].

$$i(t) = K \left[A \sin (\omega_1 t + \psi_1) + B e^{-\zeta \omega_2 t} \sin (\omega_2 t + \psi_2) \right] \tag{14}$$

where ζ is damping ratio given by (7).

$$\zeta = \frac{R}{2} \sqrt{\frac{C}{L}} \tag{15}$$

ω_2 is damping frequency as follows:

$$\omega_2 = \omega_n \sqrt{1 - \zeta^2} \tag{16}$$

ω_n is undamped natural frequency as follows:

$$\omega_n = \sqrt{\frac{1}{LC}} \tag{17}$$

Subsynchronous current induced in generator produces torque on the turbine-generator shaft. Subsynchronous torque may coincide with one of the natural frequencies of the rotary system. It causes oscillation of the shaft at some natural frequencies. Subsynchronous resonance can cause catastrophic damage to the

turbine-generator shaft. SSR is generally divided into transient and steady state which are described as follows [26].

Transient SSR occurs due to occurrence of a short circuit in a system with series compensation. Transient magnitudes include subsynchronous frequencies, which depend on elements in the network. Slip frequency f_r in generator is given by (18).

$$f_r = f_0 - f_{er} \tag{18}$$

In case this frequency coincides with one of natural frequencies of the turbine-generator rotor (f_n), torque amplitude is increased much larger with respect to the system without compensation.

Steady state (self-excitation) SSR is divided into the induction generator effect (IGE) and torsional interaction (TI). IGE considers generator as a rigid mass at constant speed connected to the network. TI considers the turbine generator with multimass shaft, which interacts with the system disturbances at its natural frequencies.

3. Power oscillation due to ferroresonance

Catastrophic circumstances and equipment failures in electrical networks are mostly caused by emerging unwanted and unpredicted phenomena in electrical network. Resonance and ferroresonance are those phenomena which have been investigated many years ago. Manitoba hydro 230 kV electrical network has experienced ferroresonant states several times. Such conditions may occur in effect of short circuit, breaker phase failure, transformer energizing, load rejection, accidental or scheduled line disconnection, and plant outage. Power oscillation has been experienced during ferroresonance studies in Manitoba hydro system. In this section, ferroresonant states, which occurred in Manitoba hydro network, are explained, and results are analyzed. The latest studies on ferroresonance in Manitoba hydro system are explained, and power oscillation due to ferroresonance is discussed in this network. In addition to that, impact of ferroresonance on electrical and mechanical parameters of hydro generator is analyzed.

3.1 Ferroresonance accidents in Manitoba hydro system

3.1.1 Failure of wound PT in effect of opening grading capacitance circuit breakers

Manitoba hydro 230 kV electrical network consists of several 230 kV power sources like Vermillion, Dorsey, Ridgway, Rosser, and Grand Rapids station. Furthermore, Ashern station comprises an overvoltage-damping reactor, and Silver station with $2 \times 230/66$ kV, YNd, 50 MVA transformers, is considered for particular ferroresonant investigations [27]. In order to meet a $-50°C$ low temperature specification, circuit breakers used in Dorsey converter station have been provided by SF6 mixed with CF4 since 1988. In high voltage systems, multiple interrupting chambers are connected in series to break the current and withstand the high recovery voltage. Grading capacitors with the values of 1500–1600 for an SF6 breaker are installed in parallel with each chamber to obtain an equal voltage distribution [28].

As shown in **Figure 2**, the 230 kV ac bus in Dorsey HVDC converter station consists of four bus sections. At 22:04, May 20, 1995, bus A2 was disconnected for maintenance. At approximately 22:30, a potential transformer (V13F) failed catastrophically. It caused damage to equipment up to 33 m away. The main reason for
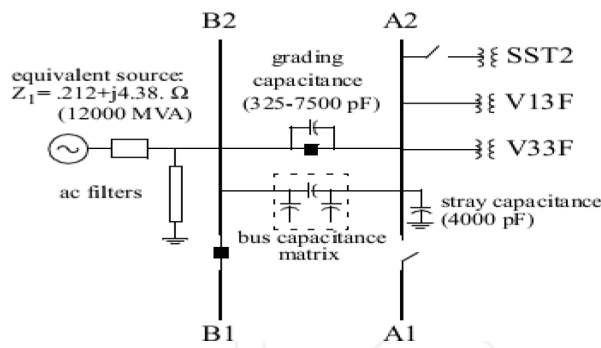
Figure 2.
Dorsey converter station 230 kV bus arrangement in Failure of wound PT.

PT explosion was occurrence of ferroresonance, which is caused by switching procedure. De-energized bus and the associated PTs were being connected to the energized bus B2 through the grading capacitors (5061 pF) of nine open 230 kV circuit breakers. Station service transformer SST2, which is normally connected to bus A2, had been previously disconnected. This arrangement leads in occurrence of ferroresonance in phase A and B [6].

3.1.2 Energizing induction motor by closing 4.16 kV circuit breaker

Another ferroresonant state occurred on August 5, 1995, at 14:18. A 4.16 kV breaker failed to latch while attempting to energize a 1500 kW induction motor at the Dorsey Converter Station [28]. It resulted in opening eleven 230 kV breakers to clear bus B2 to which the 230/4.16 kV transformer (SST1) was connected. Noise levels of SST1 were significantly higher than normal state. **Figure 3** shows bus arrangement, equivalent source impedance, and capacitances. Misshaped wave-forms and voltage increasing near 1.5 pu occurred in bus B2. This is the evidence of existing a steady-state asymmetric fundamental mode of ferroresonance.

3.2 Power oscillation due to ferroresonance examined in Manitoba hydro system

One of the popular configurations, which cause ferroresonance in the network, is transformer-terminated double circuit line. Ferroresonance occurs due to capacitive coupling between double circuit lines. In such configuration, power transformers are connected to de-energized transmission lines of remarkable length, which is parallel to another energized line.

As shown in **Figure 4**, in Manitoba hydro network, 230/66 kV transformers in Silver station are supplied from a single transmission line, which is taped from A3R line. A double circuit transmission line with a length of about 200 km comprises A3R-A4D lines, which are routed between Ashern and Rosser station. Grand Rapids is connected to Ashern station by G1A-G2A double circuit transmission line with a
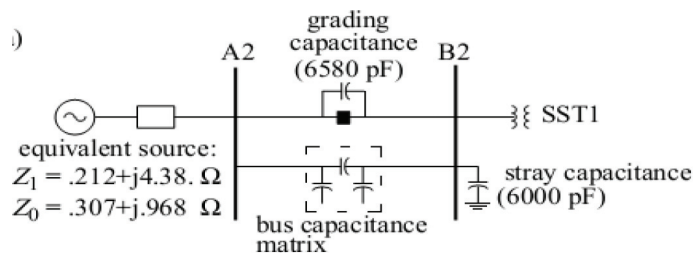

Figure 3.
Dorsey converter station 230 kV bus arrangement in closing 4.16 kV circuit breake.

length of about 234 km. Several ferroresonant states, which resulted in power oscillation, were experienced by EMTP are fully explained in [6].

New ferroresonance studies have been implemented in Manitoba hydro system to obtain other configurations vulnerable to ferroresonance in the network [9, 12]. These arrangements comprise breaker phase failure, transformer-terminated double-circuit transmission line, and plant outage. Unlike previous investigations, in obtained ferroresonant arrangements due to transformer-terminated double circuit transmission line, both lines are remained energized. Hence, it is concluded that capacitive coupling of double circuit lines is not the only reason of occurrence of ferroresonance. In the following, one of these configurations is explained.

3.2.1 Disconnection of A3R line from Rosser and G2A line from Grand Rapids station

Figure 4 shows a ferroresonant configuration in Manitoba system. In this arrangement, A3R-A4D and G2A transmission lines are energized by G1A line, which is still connected to Grand Rapids station. In addition, Vermillion is disconnected from Ashern station by a 230 kV circuit breaker in Ashern station. By such switching operation, G2A, A4D, and A3R transmission lines are changed to open-end lines. As was mentioned in advance, in order to supply transformers in Silver station, a 230 kV single line is taped from A3R line of A3R-A4D double circuit line. In such arrangement, transformers in Silver station are located at the end of an open end line whose voltage is increased.

This experiment is represented by two different conditions for a time of about 10 s. In one condition, transformers in Silver station are considered nonsaturated. As shown in **Figure 5**, the magnitude of voltage is increased up to 304 $kV_{pick\ prim}$ (pick value in primary side) in Silver station due to voltage increment in open-end line, whereas this value is 209 $kV_{pick\ prim}$ in normal status. It must be noted that all mentioned voltage and current magnitudes in this paper are phase to neutral values. Oscillograph shows that voltage and current waveforms are not misshaped and remained in sinusoidal form; hence, no ferroresonance occurs in the system. In this experiment, damping reactor in Ashern station is disconnected from the network. In addition, grading capacitor circuit breakers are open in Dorsey converter station.

In another experiment, transformer core is saturated with specified values of magnetizing parameters. Oscillograph shows occurrence of ferroresonance due to
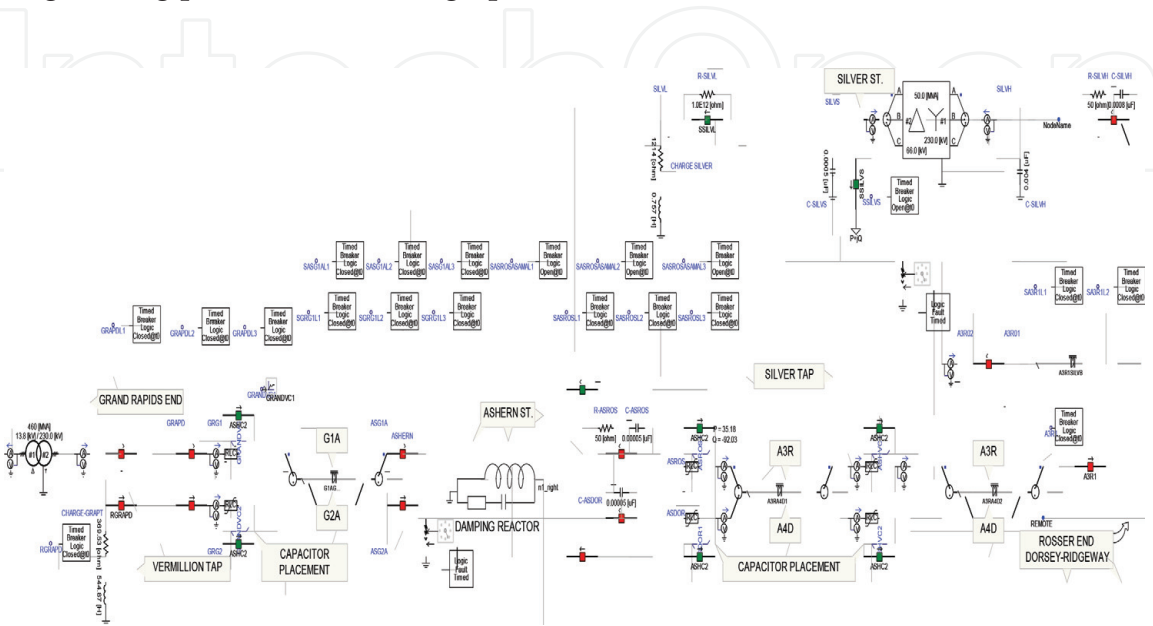

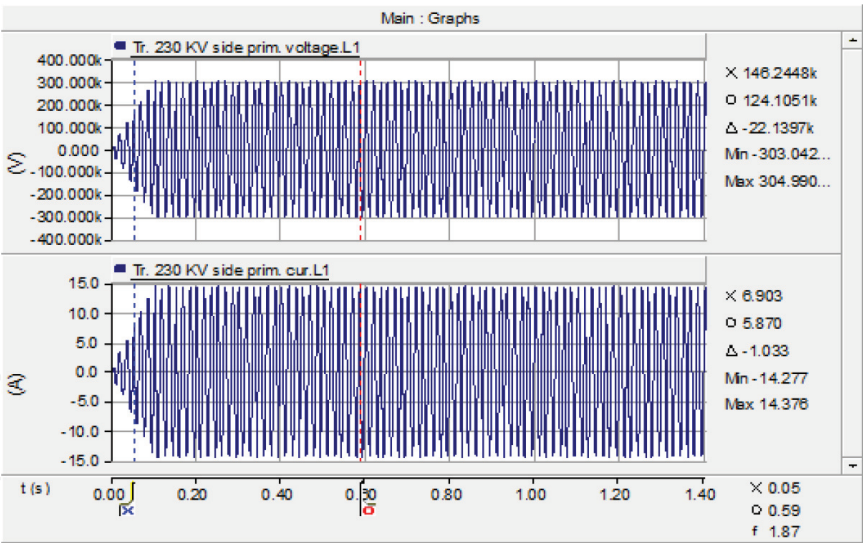**Figure 4.**
Manitoba hydro network under study in PSCAD/EMTDC.

Figure 5.
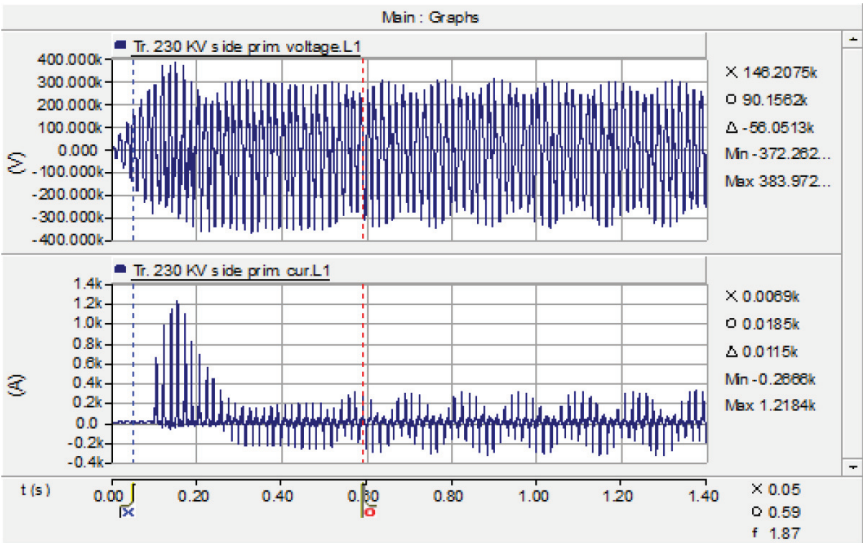*Voltage and current waveform of nonsaturated core.*

Figure 6.
Voltage and current waveform of saturated core (ferroresonance).

transformer saturation core. As shown in **Figure 6**, in addition to misshaping the waveforms, the magnitude of voltage and current is increased up to maximum values of about 383 $kV_{pick\ prim}$ and 1.21 $kA_{pick\ prim}$, respectively, at the beginning of ferroresonance.

3.3 Analysis of power oscillation in effect of ferroresonance

In fact, the main reason of occurrence of ferroresonance is existing nonlinear elements in the circuit. Consequently, the voltage and current values are nonlinear with respect to each other due to nonlinear characteristic of elements. It results in misshaping waveforms, and so that they are deviated from sinusoidal form. In such conditions, waveforms comprise orders of harmonics. It definitely depends on nonlinear characteristic of elements in the network. Frequency of total waveform is deviated from nominal frequency due to existing number of harmonics. The resulted frequency of waveform in ferroresonance depends on phase and values of orders with respect to fundamental. Reciprocally, in such conditions, frequency of

the waveform may remain in nominal value in another side of the network or can get different nonlinear characteristic. Consequently, a frequency difference between two points in the network is resulted. The main factor, which results in power oscillation, is frequency difference in the network. Frequency of power oscillation is a function of frequency difference between two points.

As was shown in **Figure 6**, voltage and current oscillate with specific period in effect of ferroresonance. Envelope of misshaped waveforms due to existing number of harmonics in ferroresonance oscillates with a frequency of about 10 Hz. It is resulted from frequency difference of about 10 Hz between Grand Rapids and Silver station.

There is significant difference between power oscillation experienced in ferroresonance and a typical oscillation in case of pole slipping in the generator. As shown in **Figure 7**, in a typical pole slipping in the generator, envelope of voltage swing advances by 180° with respect to the envelope of current swing or vice versa, whereas envelope of voltage swing is the same phase with respect to the envelope of current swing in power oscillation due to ferroresonance. Furthermore, the enve- lope of power oscillation due to ferroresonance covers negative or positive side
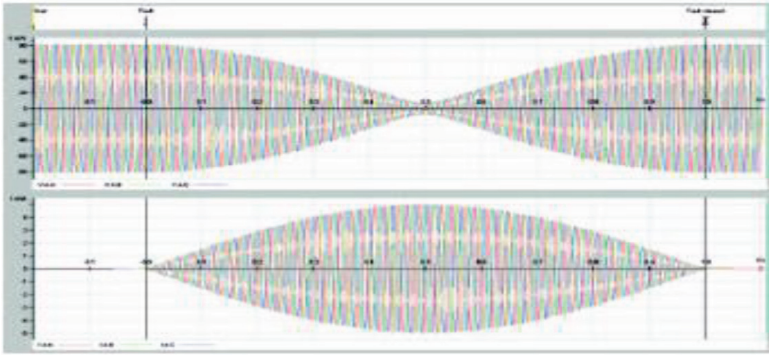

Figure 7.
Typical status of voltage and current in case of pole slipping in generator.
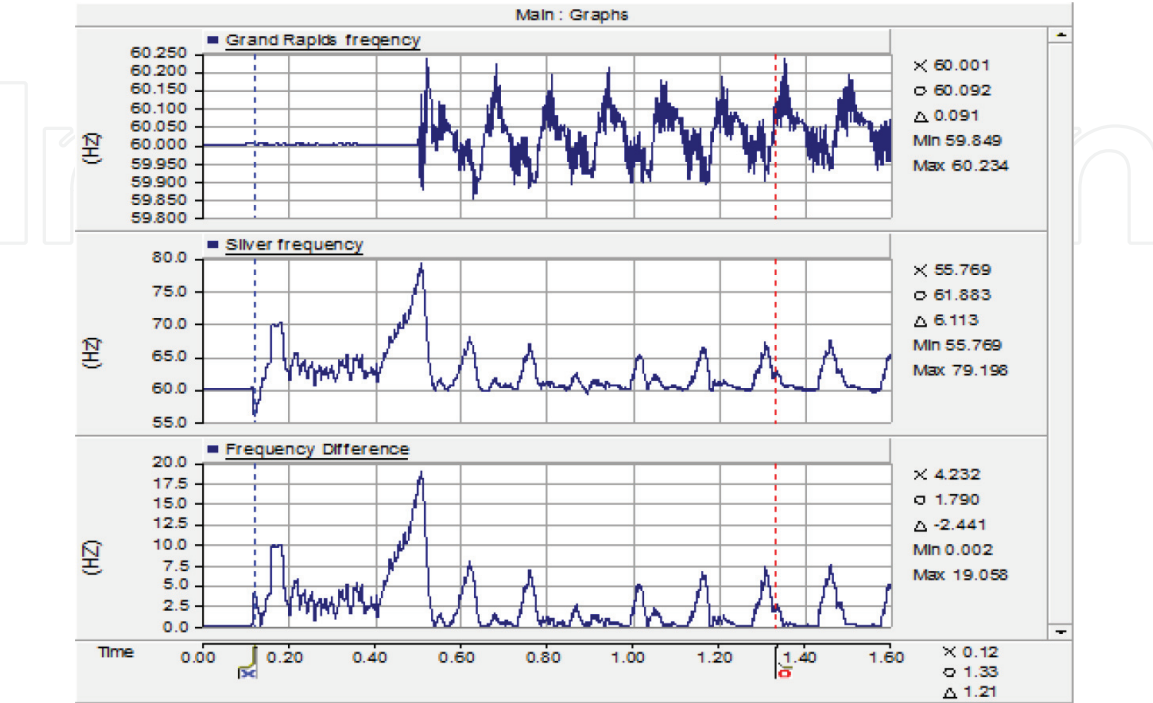

Figure 8.
Δf between Grand Rapids and Silver station.

sequentially, whereas the same envelope of power covers both negative and positive sides in each period of swing. In addition, in case of power swing in effect of out of step condition in no ferroresonant state, waveform of voltage and current mostly includes fundamental waveform. Consequently, power oscillation in case of pole slipping in the network can be distinguished from oscillation in effect of ferroresonance. It must be noted that, in some cases, electrical parameters in case of pole slipping in generator get different magnitudes and harmonic distortion according to dynamics of generator and power system.

Figure 8 shows frequency difference between Grand Rapids and Silver station during ferroresonance. As it is inferred from diagram, the frequency difference is not constant in the time of ferroresonance. Consequently, period of power oscillation is variable in such conditions.

3.4 Impact of power oscillation in effect of ferroresonance on operation of hydro generator

In order to analyze impact of power oscillation in effect of ferroresonance on operation of hydro generator, Grand Rapids station in Manitoba hydro system is simulated as both equivalent circuit and hydro-generator mode in the software. In
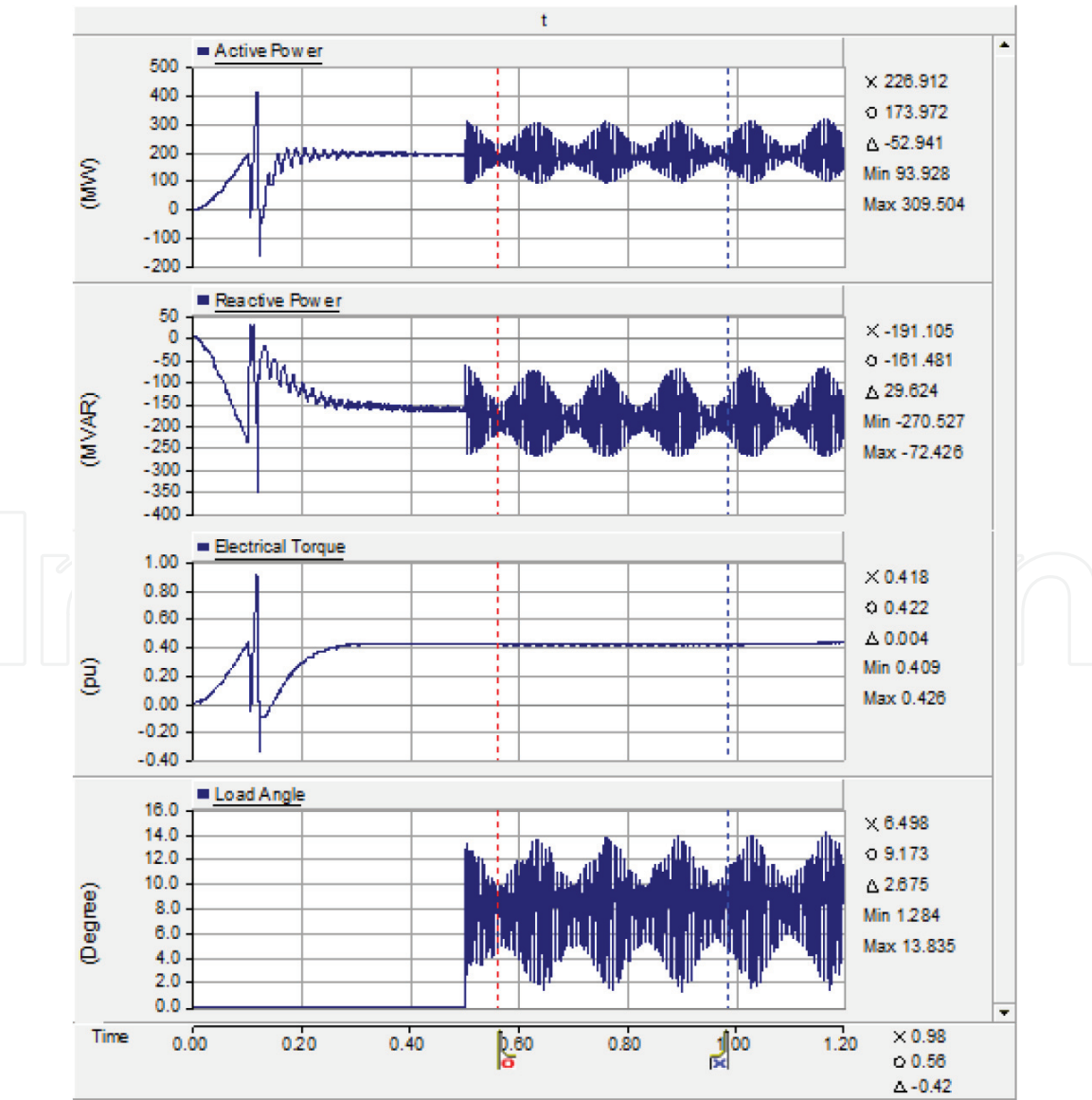

Figure 9.
Electrical parameters of hydro generator during ferroresonance.

order to compare behavior of the station in both operation mode and prevent instability due to sudden energizing at the beginning of simulation, the station is changed from equivalent circuit to hydro generator with constant speed along with exciter and PSS in the time of 0.5 s from the beginning of simulation. When the condition is stable, generator is changed to full-blown machine where governor and multi-mass torsional shaft model are also released in the time after 0.1 s. Voltage and current waveforms follow the same oscillations, as well as previous state with a lower magnitude of about 320 kV$_{\text{pick prim}}$ and 0.380 kA$_{\text{pick prim}}$, respectively, in generator mode.

Frequency difference between Grand Rapids and Silver station is about 10 Hz when station is in service as equivalent circuit. In such condition, power oscillates from 179 to 212 MW with a frequency of about 10 Hz in the time before 0.5 s.

In the time after 0.5 s (Grand Rapids in generator mode), power oscillation due to ferroresonance affects the stability of hydro generator. As shown in **Figure 9**, ferroresonance causes envelope of power with a frequency of about 16 Hz. Power oscillates increasingly from 93 to 309 MW in the time of about 3 ms in each period of envelope. Hence, frequency of power oscillation in each envelope is 166 Hz.

Electrical and mechanical parameters of hydro generator are shown in **Figures 9** and **10**, respectively. The parameters increase significantly during ferroresonance.
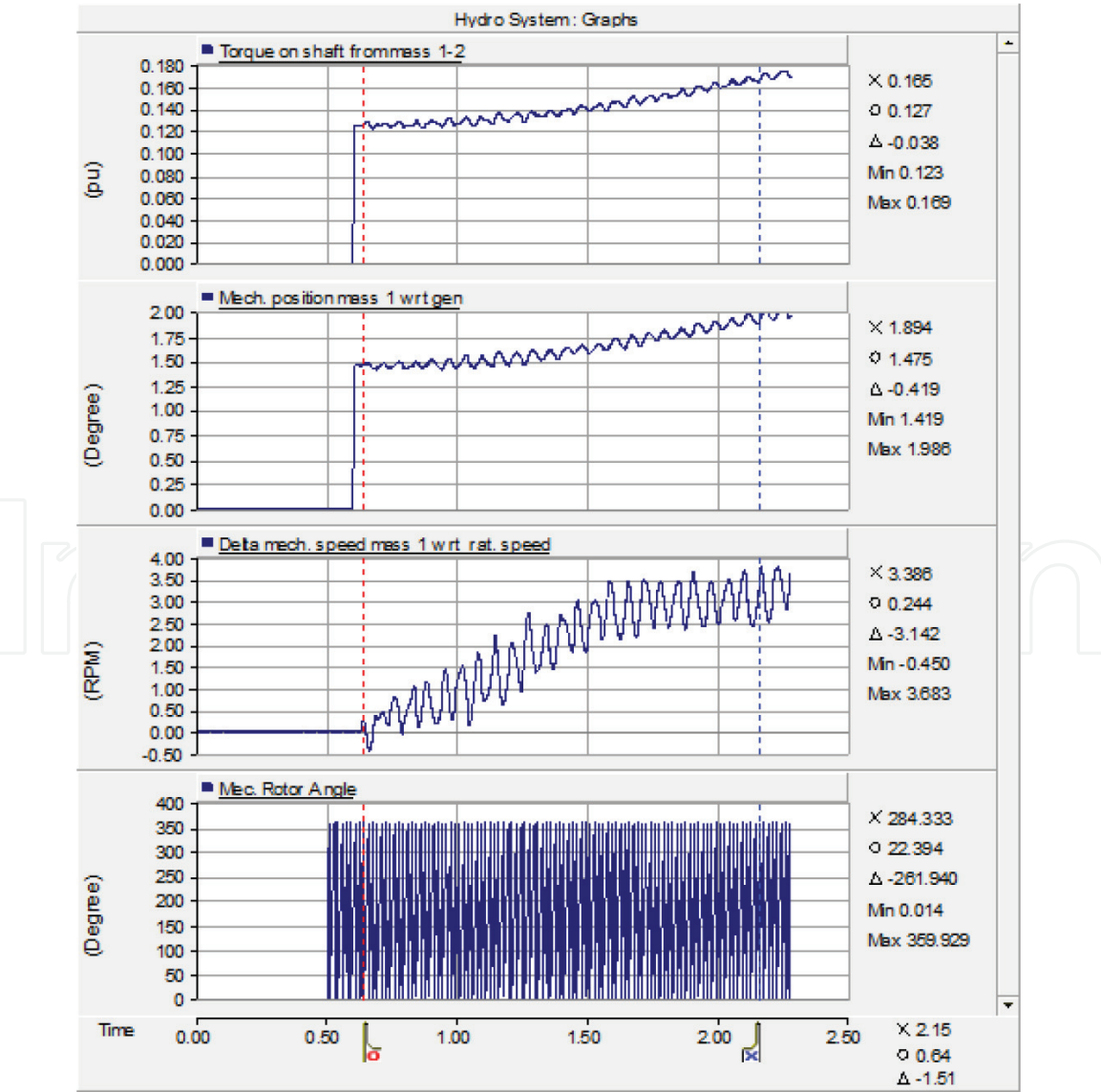

Figure 10.
Mechanical parameters of hydro generator during ferroresonance.

Hydro generator will be in unstable condition due to oscillation of parameters, which follows power oscillation in the network. Load angle oscillates as well as real power and increases up to maximum 14°; however, the value is far from power stability limit, which is defined as 90°. Mechanical parameters of the generator have increasing manner in the time of ferroresonance. Torque on shaft from generator to stage one of hydro turbine increases from 0.12 to 0.16 pu in a duration of 1.5 s. Mechanical displacement of stage 1 of hydro turbine with respect to generator increases from 1.4 to 2°. In addition, mechanical speed difference of the generator with respect to rated speed increases up to 3.6 rpm at the same time. Consequently, frequency oscillates from 59.8 to 60.2 Hz in Grand Rapids station.

4. Power oscillation due to subsynchronous resonance

The phenomenon of subsynchronous resonance on alternating self-excited power oscillation in series compensation line was first treated in the technical literature in the early of 1943. As was discussed in advance, two shaft failures occurred at the Mohave Generating Station in Southern Nevada. In this section, occurrence of SSR in Mohave power plant is explained, and test results are analyzed. Manitoba hydro system with long transmission line of about 500 km is under series compensation studies in 230 kV level. In addition to that, impact of SSR on electrical and mechanical parameters of hydro generator is analyzed.

4.1 Occurrence of subsynchronous resonance in Mohave power plant

Power generation in Mohave plant includes two 909 MVA cross-compound units. **Figure 11** shows arrangement of one unit. The high-pressure (HP) generators comprise two-pole, 483 MVA, 22 kV machines. The low-pressure (LP) generators are four-pole, 426-MVA machines each driven by LP turbine. The cross-compound units are connected to the Mohave 500 kV bus through 825 MVA, 525/22 kV transformer bank. The generation plant and its associated transmission are included into the 500 kV system, which is designed with 70% series compensation. Unit No. 2 Mohave power plant was exposed to failure in the shaft section between the generator and exciter at the main generator collector due to torsional fatigue. The mechanical strain cycling which involved plastic deformations caused the shaft to heat up to temperatures, which resulted in the breakdown of the insulation between the collector rings and the shaft. The heavy current flow that resulted from the positive and negative generator field short circuit eroded large pockets of metal from the shaft and the collector ring. Analysis of line current oscillogram taken during the disturbance on the line indicated the presence of appreciable currents of subsynchronous frequency (lower than 60 Hz).
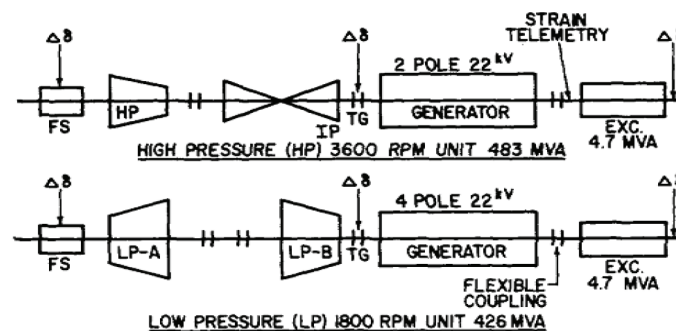

Figure 11.
Mohave generating station 909 MVA cross compound units.

Subsynchronous currents flow in the generator armature and react with the main flux of the generator to increase torque on the shaft at the slip frequency between the rotating main generator flux and the subsynchronous current flowing in the electrical network. The slip frequency following the disturbance, which causes the Mohave failures, coincided with the second flexible torsional natural frequency of the turbine-generator rotor system. It results in amplifying the magnitude of the shaft response torque. For this mode of oscillation, maximum twist occurs in the shaft span between the generator and exciter [29, 30].

4.2 Power oscillation due to SSR examined in Manitoba hydro system

As was shown in advance, Manitoba hydro system comprises G1A-G2A double circuit transmission line, which connects Ashern station to Grand Rapids station with a length of about 234 km. In another side, Ashern station is connected to Rosser station by A3R-A4D double circuit transmission line with a length of about 200 km. Transformers in Silver station are supplied from a single line, which is tapped from A3R line in a distance of about 50 km from Ashern station. As the line comprises three sections, compensation is applied at the beginning of the line in each section individually (**Figure 4**).

Electrical resonance frequency (f_{er}) generated by the elements of the network including series capacitance produces a frequency in hydro generator in Grand Rapids station. It may coincide with one of natural frequencies of the hydro generator. Rotor shaft comprises a 4-section turbine, generator, and exciter. Natural frequencies of the rotor are categorized in six torsional modes. **Table 2** shows electrical specifications of series compensation in each section. F_{er} generated by the elements of the network produce f_r, which may coincide with one of natural frequencies (f_n) of 480-MW hydro generator in Grand Rapids station. Inertia constant, shaft stiffness, and natural frequencies of rotor shaft are shown in **Table 3**.

G1A-G2A 234 km			A3R-A4D 50 km			A3R-A4D 150 km		
Comp. %	XL (Ω)	C (μf)	Comp. %	XL (Ω)	C (μf)	Comp. %	XL (Ω)	C (μf)
100	50.3	53	100	10.6	250	100	32	83
75	37.5	71	75	7.95	330	75	24	110
50	25.1	105	50	5.3	500	50	18	155
25	12.5	210	25	2.65	990	25	8	330

Table 2.
Specifications of series compensation in the network.

Inertia	Value (s)	Stiffness	Value (pu. T/rad)	F_n (Hz)	Mode
JT1	0.0830	KT1-2	18.0858	51.94	5
JT2	0.1451	KT2-3	33.1075	43.15	4
JT3	0.7864	KT3-4	51.3650	33.31	3
JT4	0.7945	KT4-Gen	68.0483	0.00	0
JGen	0.7859	KGen-Exc	2.117	20.86	1
JExc	0.0284			24.97	2

Table 3.
Values of inertia, stiffness, and natural frequencies of 480 MW hydro generator.

Natural frequencies of the rotor are calculated by eigenvalue analysis and categorized in six torsional modes as shown in **Figure 12** [31–32].

Analysis of SSR is implemented by applying a three-phase fault at 230 kV side in Silver station. Compensation level is set to 75% for all three sections. The fault occurs in the time of 1.2 s from energizing, and then it is removed after 0.2 s, where
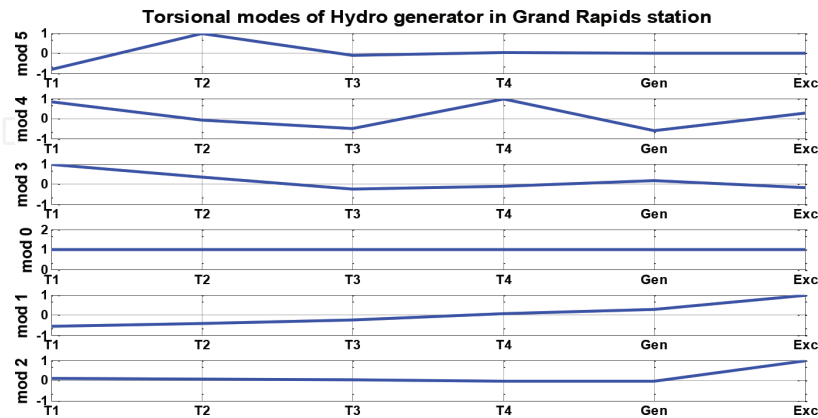

Figure 12.
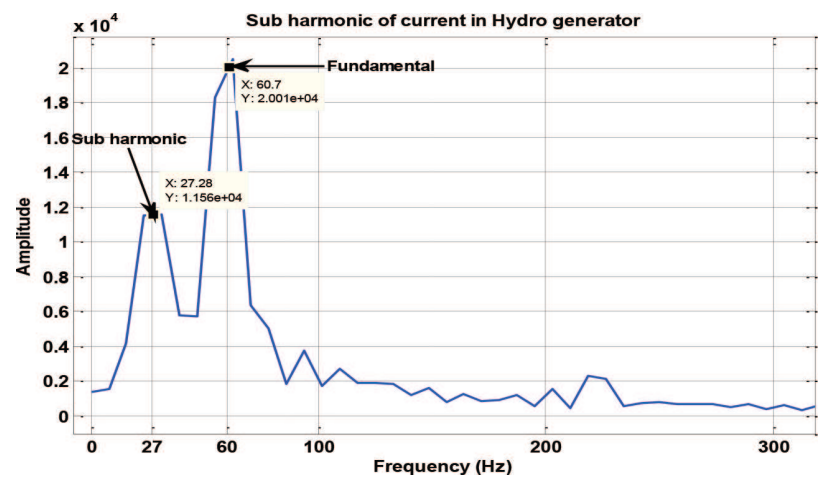*Torsional modes of hydro generator in Grand Rapids station.*

Figure 13.
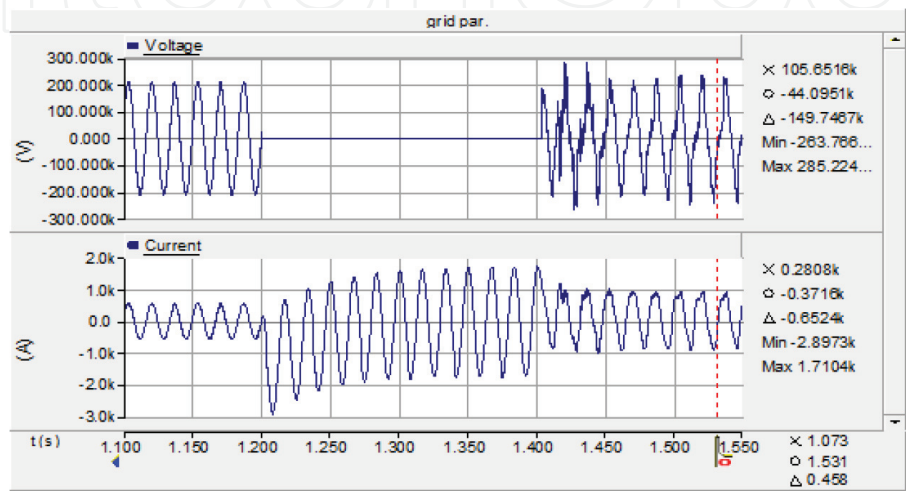*Frequency spectrum of current of generator in Grand Rapids station.*

Figure 14.
Grid parameters during short circuit in noncompensated system.
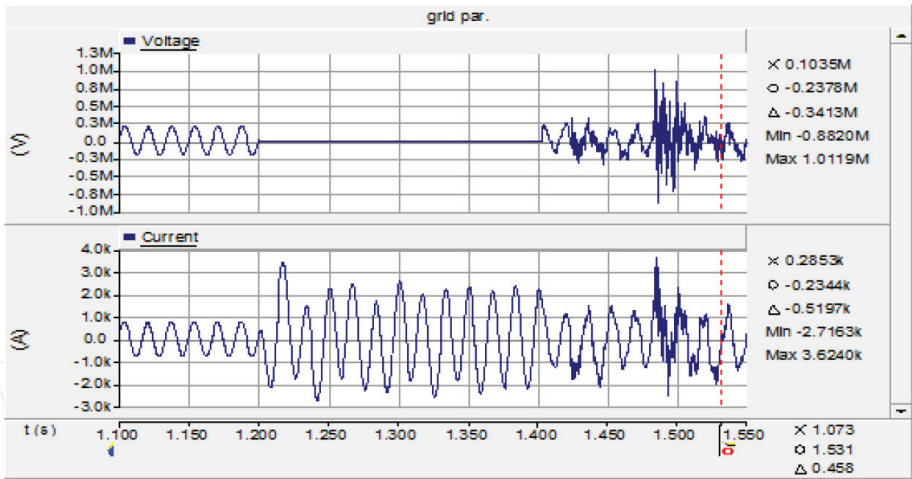
Figure 15.
Grid parameters during short circuit in series-compensated system.

Grand Rapids station is in generator mode. Current in hydro generator stator in Grand Rapids station consists of subharmonic 27 with a value of about 50% (**Figure 13**). This is f_{er}, which is generated by the network elements at the instance of short circuit. f_{er} is induced in the generator rotor and generates $f_r = 60 - 27 = 33$ Hz. The slip frequency of f_r coincides with natural frequency (**Figure 12**, mode 3) of rotor shaft in Grand Rapids station.

Figures 14 and **15** compare impact of series compensation on grid parameters with respect to noncompensated line during short circuit. As shown in **Figure 14**
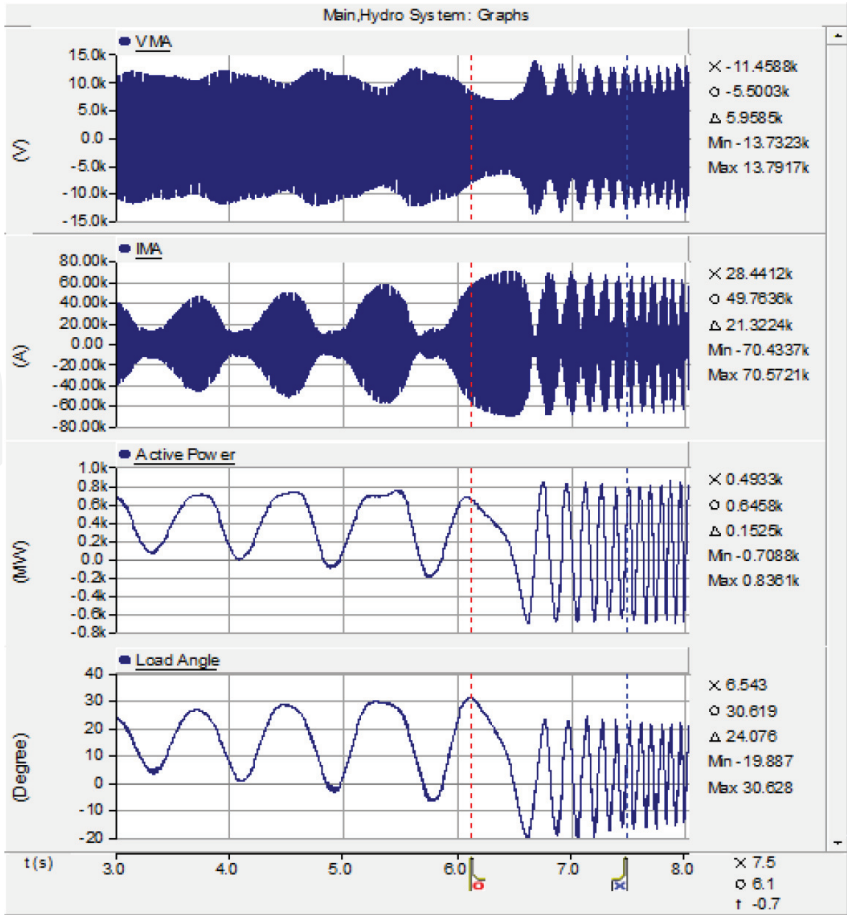

Figure 16.
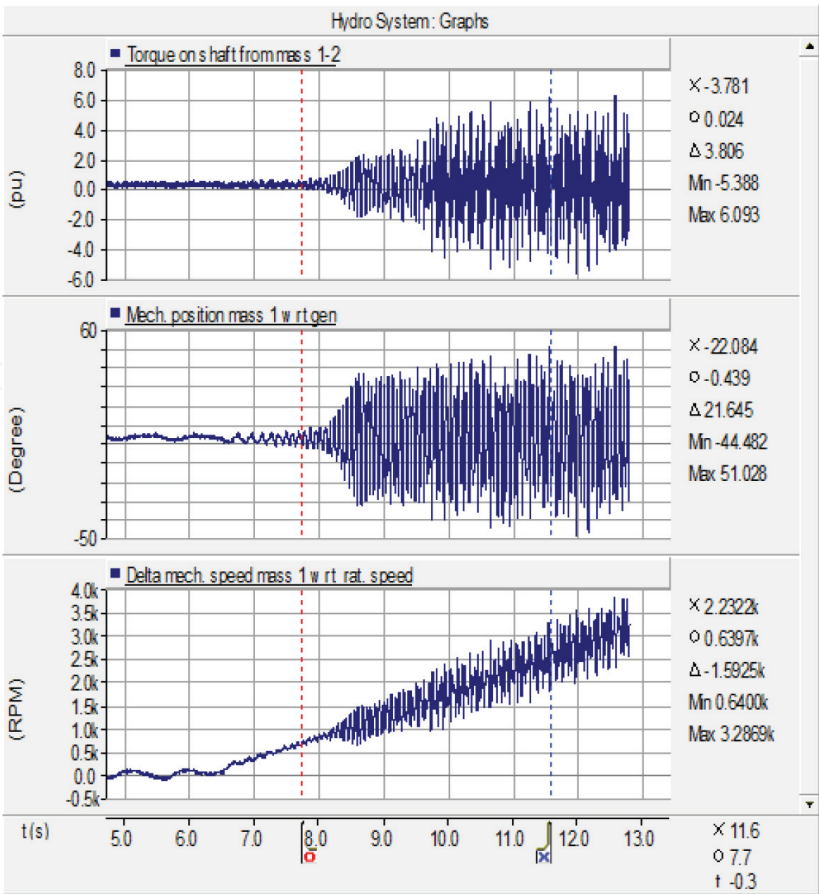*Electrical parameters of hydro generator during SSR.*

Figure 17.
Mechanical parameters of hydro generator during SSR.

(noncompensation), voltage increases up to 285 kV$_{pick}$ in two periods and suppresses immediately. Current includes DC component, which is decayed gradually. In **Figure 15**, (series compensation) voltage increases up to 1 MV$_{pick}$. It causes saturation of transformer core and occurrence of ferroresonance. Current waveform is misshaped and includes subharmonics, which flow in the network. Electrical parameters of hydro generator are shown in **Figure 16**. Active power and load angle increase and oscillate along with increasing and oscillation of voltage and current after removing the fault and power oscillation begins with a frequency of about 1.5 Hz. Envelope of current grows up to 2.66 times greater than nominal current. As shown in **Figure 17**, oscillation of active power in Grand Rapids station causes increasing and oscillation of mechanical parameters of the hydro generator. Torsional strength from turbine to generator increases significantly in the time after 9 s. Direction of torque on the shaft and mechanical displacement between turbine to generator changes alternatively and increases at the same time. In addition, speed of the masses increases significantly with respect to rated speed.

Author details

Salman Rezaei
Kerman Power Generation Management Company, Kerman, Iran

*Address all correspondence to: rezaiesalman@gmail.com

IntechOpen

References

[1] Boucherot P. Éxistence de deux régimes en ferrorésonance. Rev. Gen. de L'Éclairage Électrique. 1920;**8**(24): 827-828

[2] Ferracci P. Ferroresonance-Cahier Technique Schneider no. 190; Groupe Schneider; 1998

[3] Valverde V, Buigues G, Mazón AJ, Zamora I, Albizu I. Ferroresonant configurations in power systems. In: International Conference on Renewable Energies and Power Quality (ICREPQ'12); 28-30 March 2012, Santiago de Compostela, Spain. 2012

[4] Jacobson DAN, Lehn Peter W, Menzies W. Robert: Stability domain calculations of period-1 ferroresonance in a nonlinear resonant circuit. IEEE Transactions on Power Delivery. 2002; **17**(3):865-871

[5] Kováč M, Eleschová Ž, Heretík P, Koníček M. Analysis and mitigation of ferroresonant oscillations in power system. Proceedings of the 15th International Scientific Conference on Electric Power Engineering (EPE). 2014. pp. 211-216

[6] Jacobson DAN. Field testing, modeling, and analysis of ferroresonance in a high voltage power system [Ph.D. dissertation]. Dept. elect. and comp. Eng., Univ. Manitoba; 2000

[7] Scott LH. A case study of ferroresonance in a CCVT secondary circuit and its impact on protective relaying. In: WPRC; 17-19 October 2006; Spokane, Washington. 2006

[8] Jacobson DAN, Menzies RW. Investigation of station service transformer ferroresonance in Manitoba Hydro's 230 kV Dorsey Converter Station. In: Proc. IPST conf. Rio de Janeiro; 2001

[9] Rezaei S. Impact of plant outage on ferroresonance and mal operation of differential protection in presence of SVC in electrical network. IET Generation, Transmission and Distribution. 2017;**11**(7):1671-1682

[10] Karaagac U, Mahseredjian J, Cai L. Ferroresonance conditions in wind parks. Electric Power Systems Research. 2016;**38**:41-49

[11] Siahpoosh MK, Dorrel D, Li L, Ferroresonance assessment in a case study wind farm with 8 units of 2 MVA DFIG wind turbines. 20th International Conference on Electrical Machines and Systems (ICEMS). 2017. pp. 1-5

[12] Rezaei S. Impact of ferroresonance on protective relays in Manitoba hydro 230 kV electrical network. In: Proc. IEEE 15th Int. Conf. on Environment and Electrical Engineering. Rome, Italy; 2015. pp. 1694-1699

[13] Ballance JW, Goldberg S. Sub synchronous resonance in series compensated transmission lines. IEEE Transactions on Power Apparatus and Systems. 1973;**PAS-92**:1649-1658

[14] Varghese M, Wu FF, Varaiya P. Bifurcations associated with sub-synchronous resonance. IEEE Transactions on Power Systems. 1998; **13**(1):139-144

[15] Gupta S, Moharana A, Varma RK. Frequency scanning study of sub-synchronous resonance in power systems. In: 26th IEEE Canadian Conference on Electrical and Computer Engineering (CCECE). 2013. pp. 1-6

[16] Nagabhushana; Chandrasekharaiah BS, Lai LL, Vujatovic D. Neural network approach to identification and control of sub-synchronous resonance in series compensated systems. In: Proceedings of the IEEE Int. Conf. on Power Electronics and Drive Systems. PEDS '99. Vol. 2. 1999. pp. 683-687

[17] Yousif N, Al-Dabbagh M. Time-frequency distribution application for sub-synchronous resonance analysis in power systems. In: International Power Engineering Conference. Vol. 2. 2005. pp. 771-775

[18] Khalilinia H, Ghaisari J. Improve sub-synchronous resonance (SSR) damping using a STATCOM in the transformer bus. In: IEEE EUROCON. 2009. pp. 445-450

[19] Umre BS, Helonde JB, Modak JP, Renkey S. Application of gate-controlled series capacitors (GCSC) for reducing stresses due to sub-synchronous resonance in turbine-generator shaft. In: IEEE Energy Conversion Congress and Exposition. 2010. pp. 2300-2305

[20] Lak A, Nazarpour D, Ghahramani H. Novel methods with fuzzy logic and ANFIS controller based SVC for damping sub-synchronous resonance and low-frequency power oscillation. In: 20th Iranian Conference on Electrical Engineering (ICEE2012). 2012. pp. 450-455

[21] Mohammad pour HA, Santi E. Sub-synchronous resonance analysis in DFIG-based wind farms: Definitions and problem identification—Part I. In: IEEE Energy Conversion Congress and Exposition (ECCE). 2014. pp. 812-819

[22] Mohammad pour HA, Santi E. Optimal adaptive sub-synchronous resonance damping controller for a series-compensated doubly-fed induction generator-based wind farm. IET Renewable Power Generation. 2015; **9**(6):669-681

[23] Gagnon R, Viarouge P, Sybille G, Tourkhani E. Identification of ferroresonance as the cause of SVC instability in a degraded series compensated network. In: IEEE Power Engineering Society Winter Meeting. Vol. 2. 2000. pp. 1377-1382

[24] Woodford DA. Solving the ferroresonance problem when compensating a Dc converter station with a series capacitor. IEEE Transactions on Power Systems. 1996; **11**(3):1325-1331

[25] Anderson PM, Agrawal BL, Van Ness JE. Sub synchronous resonance in power systems. In: IEEE PES Book. 1926. p. 9

[26] Leon AE, Solsona JA. Sub synchronous interaction damping control for DFIG wind turbines. IEEE Transactions on Power Systems. 2015; **30**(1):419-428

[27] EMTP works version 2.0.2, examples, Ferro-Demo, Data case given by Jacobson DAN

[28] Jacobson DAN. Examples of ferroresonance in a high voltage power system. In: Proc. IEEE PES General Meeting. 2003. pp. 1206-1212

[29] Walker DN, Bowler CEJ, Jackson RL, Hodges DA. Results of subsynchronous resonance test at Mohave. IEEE Transactions on Power Apparatus and Systems. 1975;**94**(5):1878-1889

[30] Tweedie R, Abrams HW. Electrical features of the 1590 MW coal-slurry-supplied Mohave generating station. IEEE Transactions on Power Apparatus and Systems. 1971;**PAS 90**(2):725-735

[31] Rezaei S. Impact of sub synchronous resonance on operation of protective relays and prevention method. In: IEEE/IAS 53rd Industrial and Commercial Power Systems Technical Conference (I&CPS); 2017; Niagara Falls, ON, Canada. 2017. pp. 1-9

[32] Rezaei S. An adaptive algorithm based on sub harmonic and time domain analysis to prevent mal operation of overcurrent relay during sub synchronous resonance. IEEE Transactions on Industry Applications. 2018;**54**(3):2085-2096